MOLECULAR AND CELLULAR BIOLOGY, Aug. 2006, p. 5688–5697 Vol. 26, No. 15
0270-7306/06/$08.00+0 doi:10.1128/MCB.00779-06

GRP78/BiP Is Required for Cell Proliferation and Protecting the Inner Cell Mass from Apoptosis during Early Mouse Embryonic Development

Shengzhan Luo,† Changhui Mao,† Brenda Lee, and Amy S. Lee*

Department of Biochemistry and Molecular Biology, USC/Norris Comprehensive Cancer Center, University of Southern California Keck School of Medicine, Los Angeles, California 90089-9176

Received 3 May 2006/Accepted 6 May 2006

GRP78, also known as BiP, is a central regulator of endoplasmic reticulum (ER) homeostasis due to its multiple functional roles in protein folding, ER calcium binding, and controlling of the activation of transmembrane ER stress sensors. ER stress induction of GRP78/BiP represents a major prosurvival arm of the unfolded protein response (UPR). However, the physiological role of GRP78 in development is not known. Using a transgenic approach, we discovered that the Grp78 promoter is activated in both the trophectoderm and inner cell mass (ICM) of embryos at embryonic day 3.5 via a mechanism requiring the ER stress elements. To reveal the function of the GRP78 in vivo, we created a *tri-loxP* Grp78 mutant allele, which was further crossed with *EIIA-cre* to create a knockout allele. The *Grp78*$^{+/-}$ mice, which express 50% of the wild-type level of the GRP78 protein, are viable. Interestingly, the heterozygous Grp78 cells up-regulate the ER proteins GRP94 and protein disulfide isomerase at both the transcript and protein levels, while other UPR targets such as CHOP and XBP-1 are not affected. Further studies revealed that mouse embryonic fibroblasts from *Grp78*$^{+/-}$ mice are capable of responding to ER stress. However, *Grp78*$^{-/-}$ embryos that are completely devoid of GRP78 lead to peri-implantation lethality. These embryos do not hatch from the zona pellucida in vitro, fail to grow in culture, and exhibit proliferation defects and a massive increase in apoptosis in the ICM, which is the precursor of embryonic stem cells. These findings provide the first evidence that GRP78 is essential for embryonic cell growth and pluripotent cell survival.

The unfolded protein response (UPR), which is conserved from yeast to human, triggers multiple pathways to allow cells to respond to stress conditions that target the endoplasmic reticulum (ER) (17). The ER is the site for the synthesis of secretory and membrane proteins and lipids and is also a major intracellular calcium storage compartment. As such, ER homeostasis is critical for the survival of eukaryotic cells. The 78-kDa glucose-regulated protein GRP78, also referred to as the immunoglobulin binding protein BiP, is a stress-inducible ER chaperone that belongs to the HSP70 family (15, 27). GRP78 is composed of three domains: the ATPase domain, the peptide-binding domain, and a C-terminal domain with unknown function (21). GRP78 binds to the unfolded peptides through the peptide-binding domain and uses the energy from hydrolyzing ATP to promote proper folding and to prevent aggregation (22). GRP78 also possesses the capacity to bind Ca^{2+}, which helps to immobilize Ca^{2+} and maintain ER calcium homeostasis (26). Furthermore, GRP78 serves as a master modulator for the UPR network by binding to the ER stress sensors PERK, Ire1p, and ATF6 and inhibiting their activation (3, 43). Furthermore, due to its antiapoptotic property, stress induction of GRP78 represents an important prosurvival arm of the UPR, with implications for cancer progression, drug resistance, neuroprotection, and diabetes (16, 26, 42). Despite these advances, how essential GRP78 is for growth and development is unknown. This is particularly intriguing since mammalian cells possess an array of ER chaperones and cochaperones with potential compensatory functions for GRP78, although none of them is known to control the UPR stress sensory network like GRP78 (9, 32).

The first hint that GRP78 function is critical for eukaryotic cell function is that its amino acid sequence is highly evolutionarily conserved from yeast to human (45). We reported previously that by the criterion of two-dimensional gel electrophoresis, GRP78 is below the detection limit at the one-cell stage and is weakly detectable from the two-cell stage to the morula stage but is abundant at the blastocyst stage in the developing mouse embryo (20). This suggests a physiological need for the induction of GRP78 during the blastocyst stage. However, the function of GRP78 has not yet been tested directly in vivo. Here, we describe the use of a transgenic (TG) approach to probe the transcriptional activation of the Grp78 promoter during early development and to map the region of the promoter required for its induction. To understand GRP78 function in vivo, we generated heterozygous and knockout (KO) Grp78 mouse models. We discovered that the targeted disruption of one copy of the Grp78 gene results in a 50% reduction in the GRP78 protein level and specific upregulation of the ER proteins GRP94 and protein disulfide isomerase (PDI) at both the transcript and protein levels. However, these compensations cannot rescue *Grp78*$^{-/-}$ embryos from lethality at the peri-implantation stage. These findings provide the first evidence that GRP78 is essential for embryonic cell growth and pluripotent cell survival.

MATERIALS AND METHODS

LacZ reporter transgenic mouse models. Creation of the 3kb/LacZ and D170/LacZ transgenic mouse models has been described previously (33). D300/LacZ was created identically, with the exception that the Grp78 promoter containing the D300 mutation was used to drive LacZ expression. Whole-mount β-galactosidase (β-gal) staining of embryos at embryonic day 3.5 (E3.5) was performed as

* Corresponding author. Mailing address: Department of Biochemistry and Molecular Biology and the USC/Norris Comprehensive Cancer Center, Keck School of Medicine of the University of Southern California, Los Angeles, CA 90089-9176. Phone: (323) 865-0507. Fax: (323) 865-0094. E-mail: amylee@usc.edu.

† S.L. and C.M. contributed equally to this work.

described previously (41), and embryos were photographed with the Axioplan2 imaging system (Zeiss). All protocols for animal use and euthanasia were reviewed and approved by the University of Southern California Institutional Animal Care and Use Committee.

Generation of the *tri-loxP*-targeting vector and Grp78-targeted ES cells. A 15-kb mouse genomic DNA containing the Grp78 gene (starting from exon 2) and its 3′-adjacent sequences was isolated from a 129/Sv-derived λ FixII genomic library (a gift of Robert Maxson, University of Southern California Keck School of Medicine). A 5.8-kb NotI/HindIII fragment was subcloned into the pBluescript KS vector and used to create the Grp78 *tri-loxP*-targeting vector, which was constructed by inserting a floxed *pgk-neo* expression cassette into intron 4, a third *loxP* site into the intron 7, and a *pgk-TK* expression cassette at the 3′ end of the construct as a negative selection marker (see Fig. 2A). The NotI-linearized DNA was purified by phenol extraction and ethanol precipitation before electroporating the DNA into the 129/Sv-derived embryonic stem (ES) cells. The ES cells were subjected to G418 and ganciclovir selection, and resistant colonies were screened for homologous recombination by PCR and Southern blot analysis.

Generation of the $Grp78^{+/T}$ and $Grp78^{+/-}$ mice. The ES cells positive for homologous recombination were subjected to subcloning to achieve a higher purity of targeted ES cells. Two of the subclones were injected into C57BL/6J donor blastocysts to produce chimera founders that were identifiable by their brown coat color. Germ line transmission of the mutant allele was confirmed by mating the founders with C57BL/6 females. First, progeny bearing the *tri-loxP* Grp78 allele (+/*T*) were identified by PCR and confirmed by Southern blot. For screening of the *tri-loxP* Grp78 allele by PCR, DNA was extracted from mouse tails or ES cells as described previously (23), and the primers used were PF1 (5′ external of the targeting construct) and PR1 (junction of *neo-loxP* cassette) (see Fig. 2A). To remove the *neo* cassette and create $Grp78^{+/-}$ mice, male $Grp78^{+/T}$ mice were crossed with female *EIIA-cre* transgenic mice. The heterozygous progeny bearing a knockout Grp78 allele (deletion between *loxP1* and *loxP3*) (Fig. 2A) were mated to wild-type (WT) female mice to segregate the knockout Grp78 allele from the *EIIA-cre* transgene, resulting in heterozygous progeny ($Grp78^{+/-}$), which carry only the knockout Grp78 allele but not the *EIIA-cre* transgene. The $Grp78^{+/-}$ mice were backcrossed to C57BL/6 mice for three or more generations prior to phenotype analysis.

Genotyping of E3.5 embryos. The genotype of E3.5 embryos was determined by nested PCR. The embryos were flushed out of the uterus, as described previously (38), with Dulbecco's modified Eagle's medium (containing 10% fetal bovine serum [FBS] and 10 mM HEPES, pH 7.5) and transferred onto another dish containing fresh medium to remove maternal blood cells before each of the embryos was picked to an individual microtube. The embryos were lysed in 20 μl of lysis buffer (50 mM Tris Cl, pH 8.0, 0.5% Triton X-100, and 200 μg/ml of proteinase K) overnight at 50°C. The samples were heated at 95°C for 10 min, which was followed by PCR analysis. The primers for the nested PCR were PF2 and PR2 followed by PF3 and PR3 (WT) and PF2 and PTR followed by PF3 and PR1 (KO). In some cases, E3.5 embryos were cultured for 6 days before they were subjected to PCR genotyping. The PCR primers used for genotyping were PF1 (5′-CTTCGAATCGGCAGCAGCCAGCTTG-3′), PR1 (5′-AATGTATGC TATACGAAGTTATTTAATCG-3′), PF2 (5′-GTTGATATTGGAGGTGGGC AAACCAAG-3′), PR2 (5′-CCCAGGTCAAACACAAGGATGTTCTTC-3′), PF3 (5′-GATTTGAACTCAGGACCTTCGGAAGAGCAG-3′), PR3 (5′-GCA ATAGCAGCTGCTGTACTGTGAGGATGA-3′), PTF (5′-TCGTATAGCAT ACATTATACGAAGTTATACA-3′), and PTR (5′-TTGTTAGGGGTCGTTC ACCTAGA-3′).

In vitro culture of E3.5 embryos. Blastocysts were flushed from the uterus of $Grp78^{+/-}$ intercrosses at E3.5 and cultured on a gelatin-coated 96-well plate in ES cell medium (15% FBS, 1% penicillin and streptomycin, 1 mM sodium pyruvate, 2 mM L-glutamine, 0.1 mM nonessential amino acids, 100 μM β-mercaptoethanol, and 1000 U/ml leukemia inhibitory factor). For mechanical removal of the zona pellucida (ZP), blastocysts were cultured in vitro for 24 h, and the ZP were removed by teasing with Pasteur pipettes with finely modified tips.

Isolation, culture, and drug treatment of MEFs. Mouse embryonic fibroblasts (MEFs) were isolated from E13.5 embryos. Briefly, the embryo was washed twice in phosphate-buffered saline (PBS) after removal of the head and internal organs, disaggregated with an 18-gauge needle in 0.25% trypsin-EDTA, and incubated at 37°C for 2 to 3 min before being added Dulbecco's modified Eagle's medium with 10% FBS and 1% penicillin and streptomycin. The cells were split after 2 days in culture, and MEFs were used for experiments. For drug treatment, the cells were treated with 300 nM thapsigargin (Tg), 1.5 μg/ml tunicamycin (Tu), or 5 mM azetidine (AzC) for 16 h prior to harvest.

BrdU and TUNEL assays. For bromodeoxyuridine (BrdU) incorporation, the blastocysts were cultured overnight in vitro and treated with 10 mM BrdU for 6 h. After fixing with 70% ethanol for 30 min and permeabilizing for 1 h at room temperature in permeabilization buffer (0.1% Triton X-100, 0.1% NP-40, and 1% bovine serum albumin in PBS), the blastocysts were incubated with anti-BrdU antibody (Amersham Biosciences) at 4°C overnight and washed three times with PBS. The blastocysts were then incubated with fluorescein-conjugated secondary antibody followed by propidium iodide staining. For terminal deoxynucleotidyltransferase-mediated dUTP-biotin nick end labeling (TUNEL), the blastocysts were cultured for 24 h in vitro, and the TUNEL assay was performed with an in situ cell death detection kit (Roche Applied Sciences) according to the manufacturer's instructions. The blastocysts were subjected to DAPI (4′,6′-diamidino-2-phenylindole) staining after TUNEL staining. The embryos were examined and imaged by fluorescent and bright-field microscopy (Olympus IX70) and then subjected to PCR genotyping.

Southern blot. The BamHI-digested DNA (from ES cells or tail biopsy) was run on a 1% agarose gel at 12 V overnight. The DNA was then transferred onto a nylon membrane and immobilized by UV cross-linking. The 5′ external probe A was a 1-kb fragment upstream of the Grp78 TATA box amplified by PCR using the following primers: 5′-TACATCTCATGGTGGAAAGTGTCTGTTT GA-3′ and 5′-CATCCTCCTTCTTGTCCTCCTCCTCG-3′. The PCR product was gel purified and labeled with radioactive [^{32}P]dCTP or dATP using a Prime It II kit (Stratagene). The 3′ probe B used was a 1.2-kb BamHI/HindIII fragment at the Grp78-neighboring *Rab9p40* locus. The hybridization was performed at 65°C overnight in PerfectHyb buffer (Sigma) supplemented with 100 μg/ml of salmon sperm DNA. The membrane was then washed under low-stringency (2× SSC [1× SSC is 0.15 M NaCl plus 0.015 M sodium citrate]–1% sodium dodecyl sulfate [SDS] at 50°C), high-stringency (0.2× SSC–0.2% SDS at 65°C), and ultrastringent (0.1× SSC–0.1% SDS at 65°C) conditions for 30 min each before being exposed to a Kodak film for 24 to 72 h.

Western blot. Whole E10.5 embryos, MEFs, or pieces of liver dissected from 6-week-old mice were homogenized in radioimmunoprecipitation assay buffer (30) with a Dounce homogenizer, followed by centrifugation at 13,000 × g at 4°C for 15 min. The Western blotting was performed as described previously (31). To detect the GRP78, GRP94, and PDI proteins, an anti-KDEL antibody (1:1,000 dilution; Stressgen) was used. To detect the N-terminal fragment of GRP78, an anti-GRP78 (N20) antibody (1:500 dilution; Santa Cruz Biotechnology) was used. The mouse monoclonal anti-β-actin antibody (Sigma) was used at a 1:5,000 dilution. Both rabbit polyclonal anticalnexin and anticalreticulin antibodies (Stressgen) were used at a dilution of 1:2,000. To detect CHOP, a mouse monoclonal antibody (Santa Cruz Biotechnology) was used at a 1:1,000 dilution. To detect both the unspliced and spliced forms of XBP-1, a rabbit polyclonal antibody (Santa Cruz Biotechnology) was used at a 1:500 dilution. The Western blotting procedure was repeated two to five times.

Northern blot. Total RNAs from E10.5 embryos and MEFs were extracted, and Northern blotting was performed as described previously (34). The probes for detection of Grp78, Grp94, and GAPDH (glyceraldehyde-3-phosphate dehydrogenase) have been described previously (11). The probe used for detection of PDI was synthesized by reverse transcription-PCR (RT-PCR) with the following primers: 5′-TCTAGCAGTCAGCGGTCTGTATTCT-3′ and 5′-TACTT CTGTAGCCGCAGCAGCCCAT-3′. The probe used for detection of the Rab9-p40 gene was synthesized by RT-PCR with the following primers: 5′-CAAGCC CAGGAAAGCCACATGGTACA-3′ and 5′-TTTTGTGCCCGCTGCCACCA TCACAT-3′.

RESULTS

De novo transcription of Grp78 in blastocysts requires the ERSE. To test directly whether GRP78 expression in early mouse embryos is in part due to de novo transcription, we examined Grp78 promoter activity in vivo through a 3kb/LacZ TG mouse model bearing a *lacZ* reporter gene driven by 3 kb of the rat Grp78 promoter (Fig. 1A). The expression profile of the 3kb/LacZ transgene has been shown to faithfully represent endogenous GRP78 expression in mouse embryos at E9.5 to E11.5, where GRP78 is highly elevated in the developing heart and in somite and neural tubes (2, 33). LacZ activity, as detected by β-gal staining, was observed in both the trophectoderm (TE) and inner cell mass (ICM) of the 3kb/LacZ blastocyst (Fig. 1B). Interestingly, not all cells in the TE and ICM showed LacZ activity. This could be due to a limitation in reporter detection, or, more interestingly, only a subpopulation

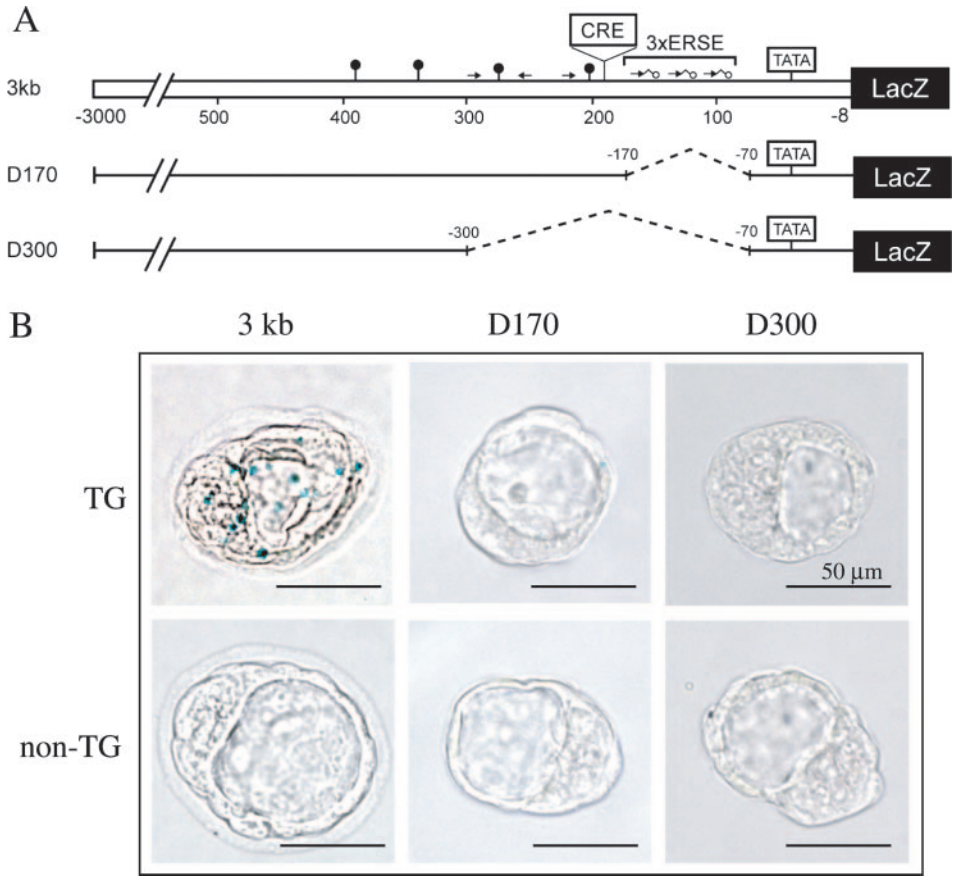

FIG. 1. High Grp78 promoter activity in blastocysts requires the ERSE. (A) Schematic representation of 3kb/LacZ and the two internal deletion mutants D170/LacZ and D300/LacZ. The locations of the TATA box, ERSE, and the CRE element are indicated. Additional CCAAT sequences and their orientations with respect to the TATA element are represented by arrows. The lollipop symbols indicate the occurrence of GC-rich sequences similar to Sp1 binding sites. The deleted regions are indicated by dashed lines. (B) Whole-mount β-gal staining of E3.5 embryos of 3kb/LacZ, D170/LacZ, and D300/LacZ TG mice and their nontransgenic (non-TG) siblings. Pictures were taken under a bright field. Scale bar, 50 μm.

of the cells was stimulated to induce GRP78. Furthermore, we observed that in the D170/LacZ TG mouse line, where the Grp78 promoter region from positions −170 to −70 containing three tandem copies of the endoplasmic reticulum stress response element (ERSE) was deleted (Fig. 1A), β-gal staining of the TE and ICM was largely eliminated (Fig. 1B). In the D300/LacZ TG mouse line where an upstream region including a CRE site was also deleted (Fig. 1A), the LacZ activity was completely abolished (Fig. 1B), although this D300/LacZ transgene was active in the adult brain (data not shown). These observations provide the first direct evidence that the Grp78 promoter is activated in both the TE and ICM cells of early developing mouse embryos, consistent with a physiological role for GRP78 in these cells. In addition, the requirement of the ERSEs for high-level Grp78 promoter activity in the mouse blastocyst raises the possibility that Grp78 induction is mediated by ER stress and UPR signaling pathways in the affected embryonic cells. These results also establish that de novo transcription of Grp78 contributes at least in part to the high level of GRP78 protein in the blastocysts.

Genetic targeting generates a Grp78 null allele. To determine whether GRP78 is essential for early development, we disrupted the Grp78 allele by gene targeting. The mouse Grp78 gene consists of eight exons (Fig. 2A). Previously, it was established that the ATPase domain contained within exons 3 through 5 is critical for the chaperone and antiapoptotic functions of GRP78 (13, 42). By taking advantage of the *cre-loxP* approach, which is capable of creating conventional as well as tissue-specific KO (24), we constructed a *tri-loxP*-targeting vector in which a floxed *neo* expression cassette was inserted at intron 4 of the Grp78 gene and a third *loxP* site was inserted at intron 7 (Fig. 2A). Targeted ES cells were used to create chimera founders. Successful germ line transmission of the targeted allele from the chimera to the progeny was screened by PCR and confirmed by Southern blotting using a probe external to the targeting vector (Fig. 2B). To generate a Grp78 null allele, the $Grp78^{+/T}$ mouse was mated with an *EIIA-cre* transgenic mouse. The *EIIA-cre* mice only express the *cre* recombinase transiently before the implantation stage during embryonic development (46), resulting in the partial excision of the region between any two of the three *loxP* sites. One of these events would delete the *neo* cassette and exons 5 through 7 that are flanked by the first and third *loxP* sites, creating a Grp78 KO allele devoid of these critical exons (Fig. 2A). The

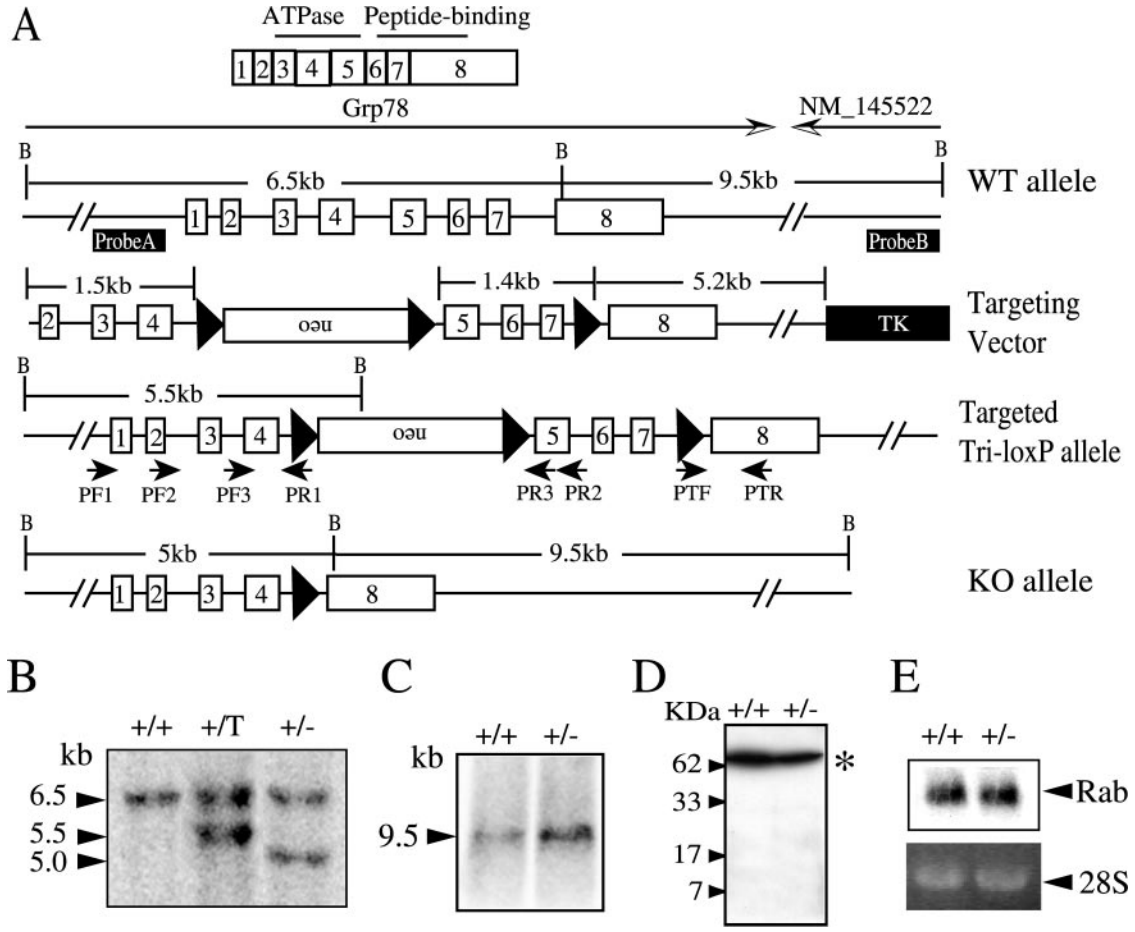

FIG. 2. Generation of Grp78 KO mice. (A) Schematic drawings for the Grp78 cDNA, the WT allele, the *tri-loxP*-targeting vector, the targeted *tri-loxP* (T), and the KO alleles. The exons encoding the ATPase domain and peptide-binding domain of GRP78, the location of the insertion of the floxed *neo* cassette, the three *loxP* sites (▶), and the *pgk-TK* expression cassette (TK) are indicated. The location of the primers [→] used in the PCR genotyping, the external 5′ probe A and the external 3′ probe B used in the Southern blot, and the BamHI restriction sites [B] are also indicated. (B) Southern blot of BamHI-digested wild-type (+/+), heterozygous $Grp78^{+/T}$, and heterozygous $Grp78^{+/-}$ DNA using the 5′ probe A. The size of each band (in kilobases) is indicated. (C) Southern blot of BamHI-digested DNA from wild-type (+/+) and $Grp78^{+/-}$ siblings, using the 3′ probe B against the 3′-adjacent Rab9p40 (Rab) gene (GenBank accession no. NM_145522). (D) Whole-cell lysates from livers of wild-type (+/+) adult mice and heterozygous $Grp78^{+/-}$ siblings were subjected to Western blot analysis with anti-GRP78 (N20) antibody. The film was overexposed to detect any truncated form of GRP78, if it exists. The asterisk indicates the 78-kDa full-length GRP78 protein. (E) Total RNA from WT (+/+) or heterozygous (+/−) E10.5 embryos were subjected to Northern blot analysis to analyze the Rab transcript level. The 28S rRNA was used as an RNA loading control.

KO allele contained within the heterozygous (+/−) progeny was first identified by PCR using different combinations of primers (data not shown) and was confirmed by Southern blotting with a probe external to the targeting vector (Fig. 2A and B). Southern blot analysis of another gene (*Rab9p40*) oriented tail to tail 2 kb downstream of the Grp78 allele showed that it is intact in the heterozygous mutant (Fig. 2C). We further determined by Western blotting that no N-terminally truncated protein was produced from the Grp78 KO allele, even when the blot was overexposed (Fig. 2D). On the other hand, Northern blotting showed similar Rab9p40 mRNA levels for the $Grp78^{+/-}$ mice and their WT siblings (Fig. 2E). Collectively, these results show that our targeting strategy has specifically created a null Grp78 allele and that disruption of the Grp78 allele does not affect its adjacent allele.

Heterozygous Grp78 cells up-regulate GRP94 and PDI. In the $Grp78^{+/-}$ mice, the GRP78 protein level in adult organs such as the liver was about 60% compared with that of the WT siblings (Fig. 3A and B). Interestingly, GRP94 and PDI levels were elevated by 1.7- and 2.1-fold, respectively, in the heterozygous mice (Fig. 3A and B). The up-regulation of GRP94 and PDI appeared to be specific since the levels of calnexin and calreticulin, two other ER chaperones processing glycoproteins, were similar in the $Grp78^{+/-}$ mice and their WT siblings (Fig. 3A and B). Similarly, in E10.5 $Grp78^{+/-}$ embryos, the level of GRP78 was about 50% of that of the WT level, and up-regulation of PDI and GRP94 was also observed (Fig. 3C and D).

MEFs from $Grp78^{+/-}$ mice are capable of responding to ER stress. To examine whether expression of GRP78 at 50% of the WT level in $Grp78^{+/-}$ cells altered their response to ER stress, MEFs were isolated from $Grp78^{+/-}$ embryos and subjected to different ER stress conditions. Consistent with the observations in vivo, $Grp78^{+/-}$ MEFs showed a lower basal

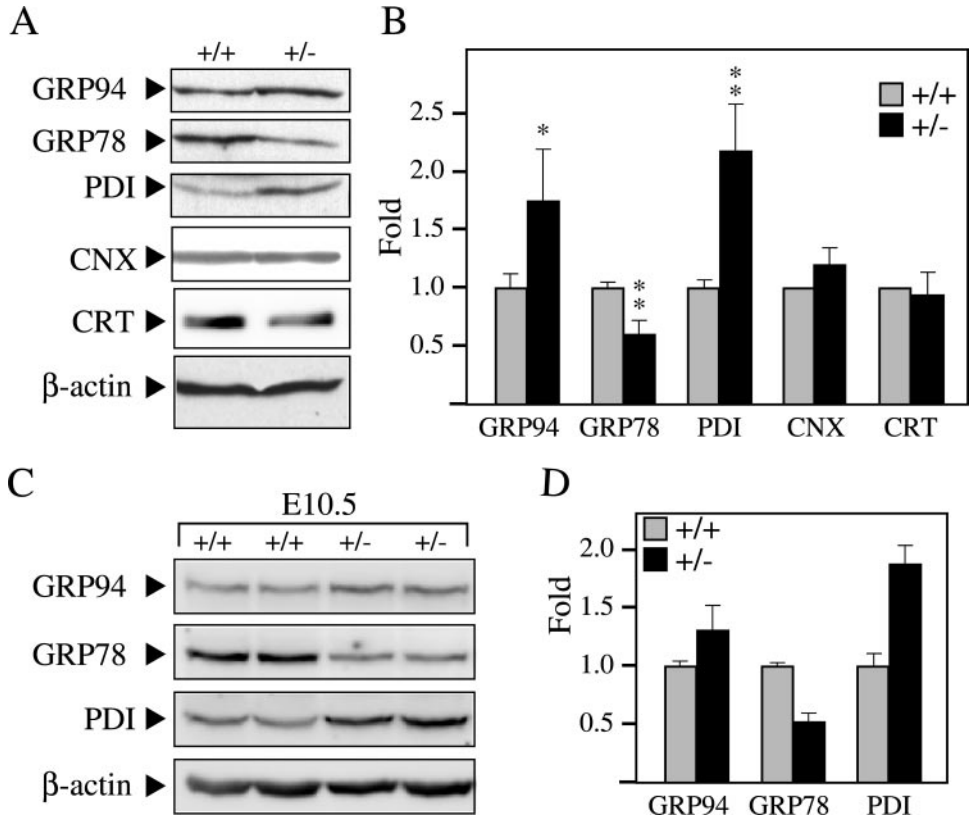

FIG. 3. Comparison of ER chaperone protein expression levels in wild-type and *Grp78*$^{+/-}$ mice. (A) Lysates from livers of WT (+/+) adult mice and *Grp78*$^{+/-}$ siblings were subjected to Western blot with anti-KDEL (detects GRP94, GRP78, and PDI), anticalnexin (CNX), anticalreticulin (CRT), and anti-β-actin antibodies. (B) Quantification of Western blot analyses performed in panel A for four pairs of mice with Quantity One software (Bio-Rad). β-Actin was used as a protein loading control. For each protein, the WT level was set as 1. The standard deviations are shown. The Student's *t* test was performed to determine the statistical significance between the wild-type (+/+) and heterozygous (+/−) levels (∗ denotes a *P* value of <0.05; ∗∗ denotes a *P* value of <0.01). (C) Lysates from E10.5 embryos of WT mice and *Grp78*$^{+/-}$ siblings were subjected to Western blot analysis with anti-KDEL and anti-β-actin antibodies. (D) Quantification of Western blots in panel C.

level of GRP78 but up-regulated basal levels of GRP94 and PDI compared with WT MEFs, while the levels of calnexin and calreticulin remained unchanged (Fig. 4A). Under various ER stress conditions such as treatment with Tg, Tu, or AzC, the protein levels of GRP78, GRP94, and PDI were induced to various extents in the *Grp78*$^{+/-}$ MEFs (Fig. 4B). The GRP78 level for the *Grp78*$^{+/-}$ MEFs under each stress condition was about 50% compared to that of WT MEFs. As expected from a higher basal level, the ER stress-induced levels of GRP94 and PDI in *Grp78*$^{+/-}$ MEFs were higher than those in WT MEFs (Fig. 4B).

We further determined that expression of GRP78 at 50% of

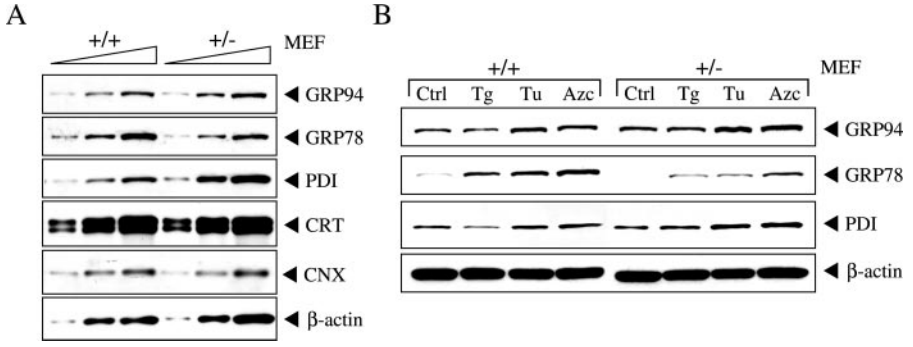

FIG. 4. Comparison of ER chaperone protein levels in wild-type and *Grp78*$^{+/-}$ MEFs. (A) Whole-cell lysates isolated from untreated WT (+/+) and *Grp78*$^{+/-}$ MEFs were subjected to Western blot analysis with anti-KDEL (detects GRP94, GRP78, and PDI), anticalnexin (CNX), anticalreticulin (CRT), and anti-β-actin antibodies. Increasing amounts (1×, 2×, and 4×) of lysates were loaded for each set. (B) Whole-cell lysates from WT (+/+) and *Grp78*$^{+/-}$ MEFs were either left untreated (Ctrl) or treated with 300 nM Tg, 1.5 μg/ml Tu, or 5 mM AzC for 16 h and subjected to Western blot analysis with anti-KDEL and anti-β-actin antibodies.

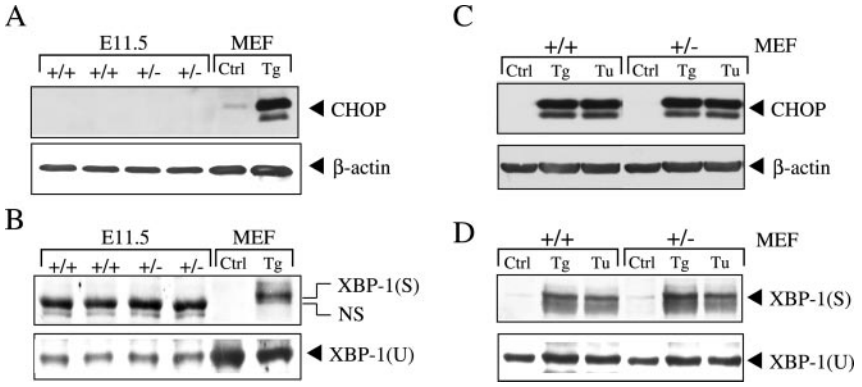

FIG. 5. Analysis of CHOP and XBP-1 activation in wild-type and *Grp78*$^{+/-}$ embryos and MEFs. (A) Lysates from WT (+/+) and *Grp78*$^{+/-}$ E11.5 embryos were subjected to Western blot analysis with anti-CHOP and anti-β-actin antibodies. WT MEFs treated with Tg were used as a positive control for CHOP induction. (B) The same blot shown in A was incubated with anti-XBP-1 antibody. MEFs treated with Tg were used as a positive control for XBP-1 splicing. The positions of the unspliced form (U) and spliced form (S) are indicated. In the embryo samples, a nonspecific (NS) band that migrated slightly faster than the spliced form was observed. (C) Lysates from WT (+/+) and *Grp78*$^{+/-}$ MEFs either left untreated (Ctrl) or treated with Tg or Tu were subjected to Western blot analysis with anti-CHOP and anti-β-actin antibodies. (D) The same blot shown in C was incubated with the anti-XBP-1 antibody. The positions of the unspliced form (U) and spliced form (S) are indicated.

the WT level in heterozygous *Grp78*$^{+/-}$ cells did not trigger the UPR signaling pathways for CHOP induction or stress-induced XBP-1 splicing. This was observed in E11.5 embryos as well as in MEFs from *Grp78*$^{+/-}$ mice grown under normal culture conditions (Fig. 5A to D). For XBP-1, both wild-type and heterozygous embryos expressed the same level of unspliced XBP-1, which was not processed into the spliced form. We noted that the spliced form of XBP-1 was distinct from a faster-migrating nonspecific band that cross-reacted with the antibody (Fig. 5B). The lack of XBP-1 splicing in both types of embryos was further confirmed by RT-PCR (data not shown). In MEFs treated with ER stress inducer Tg or Tu, both WT and heterozygous cells induced CHOP to high levels, and XBP-1 splicing was observed as expected (Fig. 5C and D). Thus, the UPR appears to be intact in *Grp78*$^{+/-}$ MEFs.

The transcript levels of GRP94 and PDI are up-regulated in heterozygous Grp78 mice and MEFs. To determine whether the increase in GRP94 and PDI protein levels in the heterozygous *Grp78*$^{+/-}$ mice is due to an increase in transcript levels, total RNA was isolated from E10.5 embryos of *Grp78*$^{+/-}$ mice, and Northern blotting was performed. Correlating with the disruption of one WT allele in the *Grp78*$^{+/-}$ mice, the level of the full-length Grp78 transcript was lower in the *Grp78*$^{+/-}$ embryos than in the WT (Fig. 6A). The KO allele gave rise to a truncated Grp78 mRNA as revealed by Western blot analysis; this truncated transcript did not result in a detectable protein (Fig. 2D). The truncated Grp78 mRNA was also observed in *Grp78*$^{+/-}$ MEFs (Fig. 6B). Furthermore, in MEFs treated with various ER stress inducers, the transcript levels of GRP94, GRP78, and PDI correlated with the protein level (Fig. 4B and Fig. 6B). This shows that the elevation of levels of GRP94 and PDI proteins in *Grp78*$^{+/-}$ embryos and MEFs is at least in part due to an increase at the transcript level. Under ER stress conditions, the heterozygous *Grp78*$^{+/-}$ MEFs were unable to compensate for the disrupted Grp78 allele at the transcript or protein level.

Grp78 null embryos fail to hatch in vitro and undergo degeneration. Although the *Grp78*$^{+/-}$ mice develop without obvious defects, they produced no *Grp78*$^{-/-}$ pups when interbred. Out of the 47 pups born, the ratio of wild-type to heterozygous to null genotypes was about 1:2:0 (Table 1). The *Grp78*$^{+/-}$ mice used for the intercross had been backcrossed to the C57BL/6 background for three or more generations, arguing against the possibility that the embryonic lethal phenotype was due to other nonspecific mutations. *Grp78*$^{-/-}$ embryos can

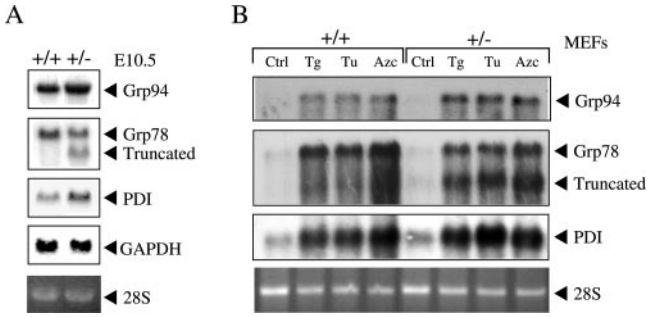

FIG. 6. Analysis of mRNA expression in wild-type and *Grp78*$^{+/-}$ mice. (A) Northern blot analysis of mRNA levels of Grp94, Grp78, and PDI in wild-type (+/+) and *Grp78*$^{+/-}$ E10.5 embryos. GAPDH and 28S rRNA were used as RNA loading controls. (B) Northern blot analysis of mRNA levels of Grp94, Grp78, and PDI in wild-type (+/+) and *Grp78*$^{+/-}$ MEFs either left untreated (Ctrl) or treated with 300 nM Tg, 1.5 μg/ml Tu, or 5 mM AzC for 16 h. 28S rRNA was used as an RNA loading control.

TABLE 1. Grp78 KO mouse[a]

Age of mouse	No. of progeny	No. of resorbed embryos	Grp78 genotype			
			+/+	+/−	−/−	ND
Postnatal	47	NA	15	32	0	
E9.5	15	4	4	7	0	
E8.5	14	2	3	9	0	
E7.5	19	4	5	10	0	
E3.5	72	NA	19	37	12	4

[a] Abbreviations: +, wild type allele; −, knockout allele; ND, could not be determined by nested PCR; NA, not applicable.

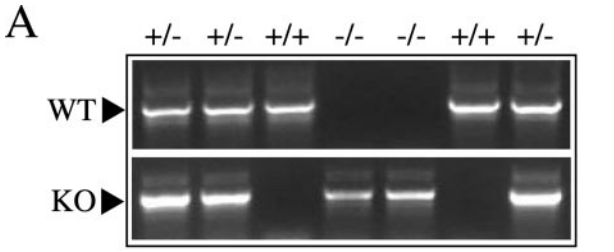

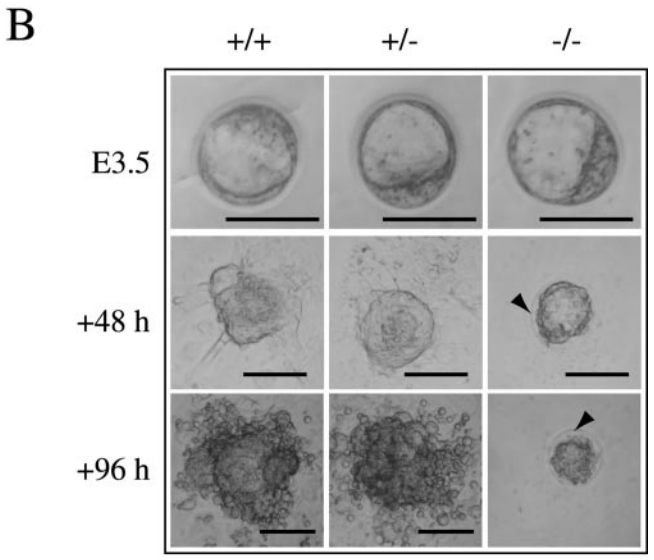

C

Genotype	Number of embryos	Number hatched
+/+	19	19
+/-	37	36
-/-	12	0
ND*	4	0

* Could not be determined by nested PCR

FIG. 7. *Grp78*$^{-/-}$ embryos do not hatch from the ZP in vitro. (A) Nested PCR of wild-type (+/+), heterozygous (+/−), and homozygous null (−/−) Grp78 alleles for E3.5 embryos. (B) Morphology of *Grp78*$^{+/+}$, *Grp78*$^{+/-}$, and *Grp78*$^{-/-}$ embryos at E3.5 and following 48 and 96 h of culture in vitro. Scale bars indicate 100 μm. The arrowheads indicate the ZP. (C) Summary of the hatching status of E3.5 embryos after 96 h of culture in vitro.

be detected at the blastocyst stage, as was shown by nested PCR genotyping of isolated E3.5 blastocysts (Fig. 7A). Among the 72 embryos examined at day 3.5, we failed to definitively determine a genotype for four of the embryos; however, from the in vitro-cultured characteristic of these four embryos discussed below, they most likely belong to the null group. This generated a ratio of 19:37:16 for the WT, heterozygous, and homozygous Grp78 null genotype, consistent with survival of the homozygous null embryos until E3.5. By day 7.5 and at later stages, no embryo bearing the null genotype was recovered; however, the existence of empty deciduas in the uterus suggests that most Grp78-deficient embryos might be able to implant in vivo, but the embryos degenerated rapidly and were resorbed (Table 1).

To investigate the cause of the lethality, 72 embryos from *Grp78*$^{+/-}$ mice intercrosses at E3.5 were cultured in ES cell medium on a gelatinized plate for 96 h and observed every 24 h before genotyping. All the WT (19 out of 19) and heterozygous (36 out of 37) embryos appeared as fully expanded blastocysts at the time of isolation, and following hatching, expansion of both ICM and TE cell types was evident after 48 h of culture in vitro, giving rise to adherent sheets of trophoblastic giant cells and outgrowth of the ICM (Fig. 7B). Strikingly, while the morphology of the E3.5 *Grp78*$^{-/-}$ embryos was normal upon isolation, 10 out of 12 failed to hatch from the ZP even after 96 h of culture in vitro, and the null blastocysts appeared to have shrunken (Fig. 7B). The remaining four embryos whose genotype could not be determined also failed to hatch and are likely to belong to the *Grp78*$^{-/-}$ group. Thus, as summarized in Fig. 7C, GRP78 deficiency leads to a failure to hatch in vitro. Additionally, the Grp78 null embryos became degenerative upon prolonged culture.

GRP78 is required for embryonic cell proliferation and protecting the inner cell mass from apoptosis. The inability of the *Grp78*$^{-/-}$ embryos to survive beyond the peri-implantation stage could be due to multiple factors including a defect in cell proliferation and expansion. To test this, the ZP of the E3.5 embryos from the *Grp78*$^{+/-}$ intercross was mechanically removed. These ZP-free embryos were then cultured in ES cell medium and examined for growth, which was followed by PCR genotyping. As expected, the WT and heterozygous embryos expanded robustly in culture, giving rise to both the ICM and TE cell types. In contrast, the homozygous Grp78 null embryonic cells were unable to expand in culture even after 5 days of culture and appeared degenerative (Fig. 8A). Upon analyzing the BrdU uptake of the E3.5 embryos after 1 day of culture, we discovered that while about 60% of the heterozygous embryonic cells showed BrdU uptake, as previously reported for embryos at this developmental stage (6), only about 7% of the Grp78 null cells showed BrdU uptake (Fig. 8B). TUNEL assays further revealed a dramatic increase in apoptosis of the ICM of the Grp78 null embryos compared to the negligible level of apoptosis in the heterozygous or WT embryos (Fig. 8C and data not shown). Thus, the lack of cell expansion of the homozygous Grp78 null embryos is likely due to a combined effect of a general proliferation defect and an increase in apoptosis of the ICM.

DISCUSSION

GRP78, a multifunctional ER protein, is involved in many cellular processes, including translocating newly synthesized polypeptides across the ER membrane, facilitating the folding and assembly of newly synthesized proteins, targeting misfolded proteins for proteasome degradation, regulating calcium homeostasis, and serving as a sensor of ER stress (12, 25, 26, 28). The recent discovery of GRP78 in the cell surface of stimulated endothelial cells and tumor cells and its require-

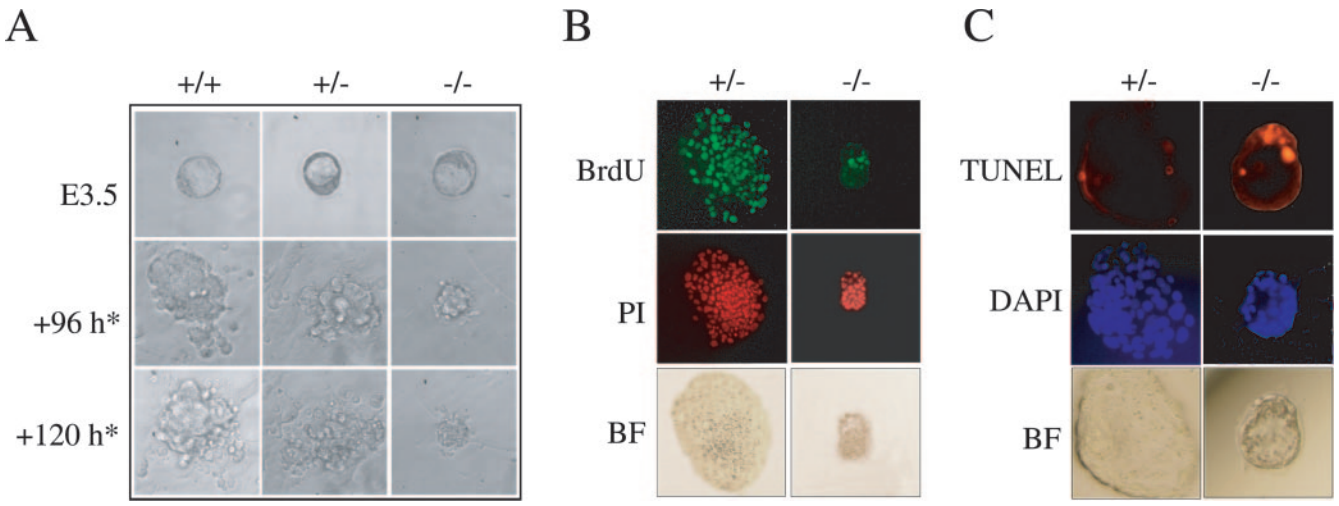

FIG. 8. *Grp78*$^{-/-}$ embryos do not grow in culture and exhibit increased apoptosis and reduced proliferation. (A) E3.5 blastocysts were isolated, and after 24 h in culture, their ZP were mechanically removed. The ZP-free embryos as indicated by an asterisk were maintained in culture for the total time indicated. Images were taken at E3.5 (upper panel), 96 h (middle panel), and 120 h (lower panel) in culture. (B) The blastocysts were cultured for 24 h in vitro, subjected to the BrdU uptake assay, and stained with anti-BrdU antibody (upper panel). The nuclei were stained by propidium iodide (PI) (middle panel). The bright-field (BF) images are also shown (lower panel). (C) TUNEL assay was performed on blastocysts after 24 h in culture (upper panel). The nuclei were stained with DAPI (middle panel), and the bright-field images were taken (lower panel). The genotypes of the E3.5 embryos are indicated on top.

ment for ligand activities further suggests a critical and novel role of GRP78 in cell surface receptor signaling pathways (1, 4, 7, 36). Despite these advances, little is known about the physiological role that GRP78 plays in development. Here, we use a combined transgenic and gene-targeting approach to probe the transcriptional regulation of the Grp78 promoter and the function of GRP78 in embryonic development. Our studies provide the first direct evidence that Grp78 is induced at the transcriptional level in both the trophectoderm and inner cell mass of E3.5 embryos and that this induction is largely dependent on the ERSE. The ERSE is the most critical transcriptional regulatory element on the Grp78 promoter mediating ER stress induction of the Grp78 promoter (26). This element is essential for the induction of the Grp78 promoter in the embryonic heart, which is achieved through synergistic interactions between the cell type-specific transcription factor GATA-4 and ERSE-binding factors ATF6 and YY1 (33, 34). Thus, during the blastocyst stage and later in embryonic mouse development, the transcriptional machinery mediated through the ERSE is activated, resulting in de novo Grp78 transcription.

To unveil the role of GRP78 during early embryonic development, we utilized a *tri-loxP* gene-targeting approach to create Grp78 mutant alleles. Studies on the Grp78 null allele, generated by crossing the *tri-loxP* Grp78 mice with the *EIIA-cre* transgenic mice, revealed several novel findings. As commonly observed for most targeted alleles, the GRP78 level is about 50% of the WT level in the *Grp78*$^{+/-}$ mice and MEFs. Nonetheless, this observation is noteworthy because the Grp78 gene is highly inducible, and it has been shown that mechanisms exist to regulate the level of GRP78 protein within the normal range. For example, CHO cells resisted the overexpression of GRP78 by down-regulating the endogenous Grp78 gene (8). Thus, the 50% expression level of GRP78 in the *Grp78*$^{+/-}$ embryos and MEFs establishes that both Grp78 alleles contribute to expression and that the compensatory mechanism to restore it to the WT level, if any, is not operational in these cells.

In the *Grp78*$^{+/-}$ mice, GRP94 and PDI are up-regulated at both the transcript and protein levels. Interestingly, the levels of other ER chaperones such as calreticulin and calnexin are not affected. These novel observations suggest that in mammalian cells, GRP78, GRP94, and PDI may be components of a functional complex or a regulatory network and that a feedback mechanism exists to sense and compensate for the drop in GRP78 levels by specifically up-regulating the other components. This up-regulation is at least in part due to an increase in the transcript level. We further determined that other UPR targets such as CHOP and XBP-1 are not activated in the same cells. However, they are readily inducible under ER stress conditions. Since the UPR appears to be intact in the *Grp78*$^{+/-}$ MEFs, the specific induction of PDI and GRP94 in the *Grp7*$^{+/-}$ embryos and MEFs likely occurs through mechanisms independent of the conventional UPR, although this remains to be proven.

Third, under ER stress conditions, both protein and mRNA levels of GRP78 for *Grp78*$^{+/-}$ MEFs are about 50% of those of the wild-type MEFs, suggesting that the copy number of the Grp78 gene is the rate-limiting factor for optimal induction of GRP78 in these cells. On the other hand, GRP94 and PDI are induced to a higher level in the *Grp78*$^{+/-}$ MEFs than in the WT MEFs, although the two types of MEFs have the same number of functional Grp94 and PDI genes. Thus, it is tempting to speculate that GRP78 not only monitors the activation of the ER stress response but may also negatively regulate specific pathways leading to the transcriptional activation of Grp94 and PDI. As nuclear localization of GRP78 has been reported previously (35, 37), GRP78 may regulate these pathways as an ER or nuclear protein. Future investigations will be required to address this interesting issue.

Our study also provides the first direct evidence that GRP78 is essential for early embryo development by targeted disruption of the Grp78 gene in the mouse. Heterozygous *Grp78*$^{+/-}$ mice showed no apparent abnormality in embryos or adults, indicating that one copy of the Grp78 gene is sufficient for normal development. Since the protein levels of PDI and GRP94 are elevated in the heterozygous *Grp78*$^{+/-}$ mice, it is possible that the apparent normal phenotype of *Grp78*$^{+/-}$ mice is in part due to these compensations. On the other hand, the lethality of *Grp78*$^{-/-}$ embryos indicates that GRP78 function is not replaceable by GRP94, PDI, or the existing complements of other cellular chaperones and members of the HSP70 protein family. We did not detect any truncated protein using an antibody derived against the N terminus of GRP78, and in addition, the *Grp78*$^{+/-}$ embryos showed no obvious defects, suggesting no gain of function for the mutant allele. Thus, it is unlikely that the phenotypes we observed with the *Grp78*$^{-/-}$ embryos are due to a dominant negative effect of the mutant alleles. Furthermore, the *Grp78*$^{+/-}$ mice used in the intercrosses had been backcrossed to the C57BL/6J background for three or more generations, further arguing against the possibility that the phenotype observed results from secondary mutations. Interestingly, we noted that the insertion of a *neo*-resistant gene cassette in the fourth intron of Grp78 is sufficient to inactivate the gene, as *Grp78*$^{T/T}$ embryos also died at around E3.5, and the GRP78 level was 50% of the WT level, while both GRP94 and PDI were up-regulated (data not shown). This phenomenon of gene inactivation has been reported for other targeted alleles, possibly through the interference of gene splicing (44). Irrespective of the mechanism, our results clearly establish that GRP78 is absolutely required for mouse embryos to grow beyond E3.5.

A likely explanation for why GRP78 is required during early development is that the peri-implantation stage may constitute physiological ER stress in its heightened activity of cell proliferation and secretion, and GRP78 controls one or more of the obligatory steps. If GRP78 is the essential chaperone for the translocation of proteins into the ER lumen as in the case for yeast cells, its elimination will result in a severe deficiency in ER protein synthesis, membrane receptor assembly, and secretion of enzymes and growth factors. Thus, deficiencies in processing and/or secretion of tryptases involved in blastocyst hatching and outgrowth could impede *Grp78*$^{-/-}$ embryos from hatching and expanding in culture in vitro (39). Likewise, the failure to process cell surface growth factor receptors may also explain the proliferative defect. Our finding that cell replication in the ICM is substantially reduced in homozygous Grp78 null embryos further suggests that GRP78 itself and/or its client proteins are essential for pluripotent cell proliferation. Thus, GRP78 provides a novel model system for the elucidation of interactive protein partners and pathways that may contribute to embryonic stem cell growth and survival, which have important implications for human stem cell therapy (19).

Interestingly, within the environment of the uterus and in the presence of other hatching embryos, most *Grp78*$^{-/-}$ embryos are apparently able to hatch and implant; however, the embryos quickly degenerated, giving rise to empty deciduas. We demonstrate here that embryos devoid of GRP78 exhibit a substantial increase in apoptosis of the ICM. Since GRP78 is known to suppress ER stress signaling, complete elimination of GRP78 could lead to the inadvertent activation of proapoptotic pathways from the ER (3, 25, 29). GRP78 can also directly interfere with components of the apoptotic pathways (29, 40, 42). It is also possible that the failure to process and secrete blastocyst antiapoptotic factors such as transforming growth factor α and gonadotropin-releasing hormone I may lead to an increase in apoptosis (5, 18).

The role of GRP78 most likely expands beyond early development. In support of this notion, high levels of GRP78 were detected in the heart, somite, and neural tube of developing mouse embryos at day 9.5 and day 10.5 (2). Elevated levels of GRP78 in the testes also imply that GRP78 might play an important role in spermatogenesis (14). In addition, Grp78 may be crucial for B-cell maturation because of its role in antibody synthesis (10). It was recently reported that genetic disruption of SIL1/BAP, which encodes an adenosine nucleotide exchange factor of GRP78, leads to protein accumulation, ER stress, and subsequent neurodegeneration (47). While this strongly implicates GRP78 in neuroprotection, our finding that a Grp78 deficiency results in early embryonic lethality further reveals that SIL/BAP is not an obligatory cochaperone for GRP78 during early development. Mice homozygous for the floxed Grp78 allele in which partial Cre-mediated recombination resulted in selective excision of the Neo resistance cassette are viable and express GRP78 normally (our unpublished results). These mice will be suitable for future investigations to generate conditional knockout models of GRP78. This will help to reveal the functional role of GRP78 throughout development and in diseases (28).

ACKNOWLEDGMENTS

We thank Steven Rawlings for the isolation and initial characterization of Grp78 genomic clones and Dezheng Dong for technical assistance. We thank Chyun-Sheng Lin at the Columbia University Transgenic Facility for the generation of targeted ES cells and Liqiong Liu, Nancy Wu, and Youzhen Yan of the USC/Norris Comprehensive Cancer Center Transgenic/Knockout Facility for the generation of the mouse models. We thank Robert Maxson and Frank Constantini for helpful discussions.

This work was supported in part by National Cancer Institute grant CA27607 (A.S.L.).

REFERENCES

1. **Arap, M. A., J. Lahdenranta, P. J. Mintz, A. Hajitou, A. S. Sarkis, W. Arap, and R. Pasqualini.** 2004. Cell surface expression of the stress response chaperone GRP78 enables tumor targeting by circulating ligands. Cancer Cell **6:**275–284.
2. **Barnes, J. A., and I. W. Smoak.** 2000. Glucose-regulated protein 78 (GRP78) is elevated in embryonic mouse heart and induced following hypoglycemic stress. Anat. Embryol. **202:**67–74.
3. **Bertolotti, A., Y. Zhang, L. M. Hendershot, H. P. Harding, and D. Ron.** 2000. Dynamic interaction of BiP and ER stress transducers in the unfolded-protein response. Nat. Cell Biol. **2:**326–332.
4. **Bhattacharjee, G., J. Ahamed, B. Pedersen, A. El-Sheikh, N. Mackman, W. Ruf, C. Liu, and T. S. Edgington.** 2005. Regulation of tissue factor-mediated initiation of the coagulation cascade by cell surface grp78. Arterioscler. Thromb. Vasc. Biol. **25:**1737–1743.
5. **Brison, D. R., and R. M. Schultz.** 1997. Apoptosis during mouse blastocyst formation: evidence for a role for survival factors including transforming growth factor alpha. Biol. Reprod. **56:**1088–1096.
6. **Chen, P.-L., F. Liu, S. Cai, X. Lin, A. Li, Y. Chen, B. Gu, E. Y.-H. P. Lee, and W.-H. Lee.** 2005. Inactivation of CtIP leads to early embryonic lethality mediated by G_1 restraint and to tumorigenesis by haploid insufficiency. Mol. Cell. Biol. **25:**3535–3542.
7. **Davidson, D. J., C. Haskell, S. Majest, A. Kherzai, D. A. Egan, K. A. Walter, A. Schneider, E. F. Gubbins, L. Solomon, Z. Chen, R. Lesniewski, and J. Henkin.** 2005. Kringle 5 of human plasminogen induces apoptosis of endothelial and tumor cells through surface-expressed glucose-regulated protein 78. Cancer Res. **65:**4663–4672.

8. **Dorner, A. J., L. C. Wasley, and R. J. Kaufman.** 1992. Overexpression of GRP78 mitigates stress induction of glucose regulated proteins and blocks secretion of selective proteins in Chinese hamster ovary cells. EMBO J. **11:**1563–1571.
9. **Ellgaard, L., M. Molinari, and A. Helenius.** 1999. Setting the standards: quality control in the secretory pathway. Science **286:**1882–1888.
10. **Gass, J. N., N. M. Gifford, and J. W. Brewer.** 2002. Activation of an unfolded protein response during differentiation of antibody-secreting B cells. J. Biol. Chem. **277:**49047–49054.
11. **Gazit, G., J. Lu, and A. S. Lee.** 1999. De-regulation of GRP stress protein expression in human breast cancer cell lines. Breast Cancer Res. Treat. **54:**135–146.
12. **Hendershot, L. M.** 2004. The ER function BiP is a master regulator of ER function. Mt. Sinai J. Med. **71:**289–297.
13. **Hendershot, L. M., J. Y. Wei, J. R. Gaut, B. Lawson, P. J. Freiden, and K. G. Murti.** 1995. In vivo expression of mammalian BiP ATPase mutants causes disruption of the endoplasmic reticulum. Mol. Biol. Cell **6:**283–296.
14. **Huo, R., Y. F. Zhu, X. Ma, M. Lin, Z. M. Zhou, and J. H. Sha.** 2004. Differential expression of glucose-regulated protein 78 during spermatogenesis. Cell Tissue Res. **316:**359–367.
15. **Jolly, C., and R. I. Morimoto.** 2000. Role of the heat shock response and molecular chaperones in oncogenesis and cell death. J. Natl. Cancer Inst. **92:**1564–1572.
16. **Kaufman, R. J.** 2002. Orchestrating the unfolded protein response in health and disease. J. Clin. Investig. **110:**1389–1398.
17. **Kaufman, R. J.** 1999. Stress signaling from the lumen of the endoplasmic reticulum: coordination of gene transcriptional and translational controls. Genes Dev. **13:**1211–1233.
18. **Kawamura, K., J. Fukuda, J. Kumagai, Y. Shimizu, H. Kodama, A. Nakamura, and T. Tanaka.** 2005. Gonadotropin-releasing hormone I analog acts as an antiapoptotic factor in mouse blastocysts. Endocrinology **146:** 4105–4116.
19. **Keller, G.** 2005. Embryonic stem cell differentiation: emergence of a new era in biology and medicine. Genes Dev. **19:**1129–1155.
20. **Kim, S. K., Y. K. Kim, and A. S. Lee.** 1990. Expression of the glucose-regulated proteins (GRP94 and GRP78) in differentiated and undifferentiated mouse embryonic cells and the use of the GRP78 promoter as an expression system in embryonic cells. Differentiation **42:**153–159.
21. **King, L. S., M. Berg, M. Chevalier, A. Carey, E. C. Elguindi, and S. Y. Blond.** 2001. Isolation, expression, and characterization of fully functional nontoxic BiP/GRP78 mutants. Protein Expr. Purif. **22:**148–158.
22. **Kleizen, B., and I. Braakman.** 2004. Protein folding and quality control in the endoplasmic reticulum. Curr. Opin. Cell Biol. **16:**343–349.
23. **Laird, P. W., A. Zijderveld, K. Linders, M. A. Rudnicki, R. Jaenisch, and A. Berns.** 1991. Simplified mammalian DNA isolation procedure. Nucleic Acids Res. **19:**4293.
24. **Le, Y., and B. Sauer.** 2000. Conditional gene knockout using cre recombinase. Methods Mol. Biol. **136:**477–485.
25. **Lee, A. S.** 2005. The ER chaperone and signaling regulator GRP78/BiP as a monitor of endoplasmic reticulum stress. Methods **35:**373–381.
26. **Lee, A. S.** 2001. The glucose-regulated proteins: stress induction and clinical applications. Trends Biochem. Sci. **26:**504–510.
27. **Lee, A. S.** 1992. Mammalian stress response: induction of the glucose-regulated protein family. Curr. Opin. Cell Biol. **4:**267–273.
28. **Li, J., and A. S. Lee.** 2006. Stress induction of GRP78/BiP and its role in cancer. Curr. Mol. Med. **6:**45–54.
29. **Li, J., B. Lee, and A. S. Lee.** 2006. Endoplasmic reticulum stress-induced apoptosis: multiple pathways and activation of p53-up-regulated modulator of apoptosis (PUMA) and NOXA by p53. J. Biol. Chem. **281:**7260–7270.
30. **Li, M., P. Baumeister, B. Roy, T. Phan, D. Foti, S. Luo, and A. S. Lee.** 2000. ATF6 as a transcription activator of the endoplasmic reticulum stress element: thapsigargin stress-induced changes and synergistic interactions with NF-Y and YY1. Mol. Cell. Biol. **20:**5096–5106.
31. **Luo, S., and A. S. Lee.** 2002. Requirement of the p38 MAPK signaling pathway for the induction of Grp78/BiP by azetidine stress: ATF6 as a target for stress-induced phosphorylation. Biochem. J. **366:**787–795.
32. **Ma, Y., and L. M. Hendershot.** 2004. ER chaperone functions during normal and stress conditions. J. Chem. Neuroanat. **28:**51–65.
33. **Mao, C., D. Dong, E. Little, S. Luo, and A. S. Lee.** 2004. Transgenic mouse models for monitoring endoplasmic reticulum stress in vivo. Nat. Med. **10:**1013–1014.
34. **Mao, C., W. C. Tai, Y. Bai, C. Poizat, and A. S. Lee.** 2006. In vivo regulation of Grp78/BiP transcription in the embryonic heart: role of the endoplasmic reticulum stress response element and GATA-4. J. Biol. Chem. **281:**8877–8887.
35. **Matsumoto, A., and P. C. Hanawalt.** 2000. Histone H3 and heat shock protein GRP78 are selectively cross-linked to DNA by photoactivated gilvocarcin V in human fibroblasts. Cancer Res. **60:**3921–3926.
36. **Misra, U. K., T. Sharma, and S. V. Pizzo.** 2005. Ligation of cell surface-associated glucose-regulated protein 78 by receptor-recognized forms of alpha2-macroglobulin: activation of p21-activated protein kinase-2-dependent signaling in murine peritoneal macrophages. J. Immunol. **175:**2525–2533.
37. **Morris, J. A., A. J. Dorner, C. A. Edwards, L. M. Hendershot, and R. J. Kaufman.** 1997. Immunoglobulin binding protein (BiP) function is required to protect cells from endoplasmic reticulum stress but is not required for the secretion of selective proteins. J. Biol. Chem. **272:**4327–4334.
38. **Nagy, A., M. Gertsenstein, K. Vintersten, and R. Behringer.** 2003. Manipulating the mouse embryo: a laboratory manual, 3rd ed. Cold Spring Harbor Laboratory Press, Cold Spring Harbor, N.Y.
39. **O'Sullivan, C. M., S. L. Rancourt, S. Y. Liu, and D. E. Rancourt.** 2001. A novel murine tryptase involved in blastocyst hatching and outgrowth. Reproduction **122:**61–71.
40. **Rao, R. V., S. Castro-Obregon, H. Frankowski, M. Schuler, V. Stoka, G. del Rio, D. E. Bredesen, and H. M. Ellerby.** 2002. Coupling endoplasmic reticulum stress to the cell death program. An Apaf-1-independent intrinsic pathway. J. Biol. Chem. **277:**21836–21842.
41. **Reddy, R. K., L. Dubeau, H. Kleiner, T. Parr, P. Nichols, B. Ko, D. Dong, H. Ko, C. Mao, J. DiGiovanni, and A. S. Lee.** 2002. Cancer-inducible transgene expression by the Grp94 promoter: spontaneous activation in tumors of various origins and cancer-associated macrophages. Cancer Res. **62:**7207–7212.
42. **Reddy, R. K., C. Mao, P. Baumeister, R. C. Austin, R. J. Kaufman, and A. S. Lee.** 2003. Endoplasmic reticulum chaperone protein GRP78 protects cells from apoptosis induced by topoisomerase inhibitors: role of ATP binding site in suppression of caspase-7 activation. J. Biol. Chem. **278:**20915–20924.
43. **Shen, J., X. Chen, L. Hendershot, and R. Prywes.** 2002. ER stress regulation of ATF6 localization by dissociation of BiP/GRP78 binding and unmasking of Golgi localization signals. Dev. Cell **3:**99–111.
44. **Sun, X., M. Lewandoski, E. N. Meyers, Y. H. Liu, R. E. Maxson, Jr., and G. R. Martin.** 2000. Conditional inactivation of Fgf4 reveals complexity of signalling during limb bud development. Nat. Genet. **25:**83–86.
45. **Ting, J., and A. S. Lee.** 1988. Human gene encoding the 78,000-dalton glucose-regulated protein and its pseudogene: structure, conservation, and regulation. DNA **7:**275–286.
46. **Xu, X., C. Li, L. Garrett-Beal, D. Larson, A. Wynshaw-Boris, and C. X. Deng.** 2001. Direct removal in the mouse of a floxed neo gene from a three-loxP conditional knockout allele by two novel approaches. Genesis **30:**1–6.
47. **Zhao, L., C. Longo-Guess, B. S. Harris, J. W. Lee, and S. L. Ackerman.** 2005. Protein accumulation and neurodegeneration in the woozy mutant mouse is caused by disruption of SIL1, a cochaperone of BiP. Nat. Genet. **37:**974–979.